Springer

KSME

Journal of Mechanical Science and Technology 24 (10) (2010) 1975~1980

www.springerlink.com/content/1738-494x
DOI 10.1007/s12206-010-0708-6

# Analysis of water hammer in pipelines by partial fraction expansion of transfer function in frequency domain †

Jun-Shin Lee[1,*], Bong-Ki Kim[2] Wook-Ryun Lee[1] and Ki-Yong Oh[1]

[1]*Green Growth Laboratory, Research Institute of Korea Electric Power Corporation, Daejeon 305-760, Korea*
[2]*System Dynamics Department, Korea Institute of Machinery and Materials, Daejeon 305-343, Korea*

(Manuscript Received June 13, 2010; Revised June 22, 2010; Accepted June 28, 2010)

**Abstract**

Understanding water hammer is very important to the prevention of excessive pressure build-up in pipelines. Many researchers have studied this phenomenon, drawing effective solutions through the time- and frequency-domain approaches. For the purposes of enhancing the advantages of the frequency-domain approach and, thereby, rendering investigations of the dynamic characteristics of pipelines more effective, we propose partial fraction expansion of the transfer function between the unsteady flow source and a given section. We simulate the proposed approach using a vibration element inserted into a simple pipeline, deducing much useful physical information pertaining to pipeline design. We conclude that locating the resonance of the vibration element between the first and second resonances of the pipeline can mitigate the excessive pressure build-up attendant on the occurrence of water hammer. Our method of partial fraction expansion is expected to be useful and effective in analyses of unsteady flows in pipelines.

*Keywords*: Design of pipeline; Water hammer; Frequency-domain analysis; Partial fraction expansion; Piston-type accumulator; Bladder-type accumulator

## 1. Introduction

Water hammer occurs when rapid valve closure very suddenly blocks water flow in pipelines. A water hammer's pressure wave can cause major problems ranging from noise and vibration to pipe collapse. A thorough understanding of water hammer is indispensible to prediction, avoidance or control of potentially very damaging physical phenomena in pipelines.

The governing equation of unsteady flow in pipelines is based on the continuity and momentum of the compressible fluid. The time-domain or frequency-domain approach is available for prediction of the pressure wave at a given section. The method of characteristics (MOC), one of the time-domain approaches, is most favored in that it is straightforward, accurate and numerically efficient [1, 2]. However, with conventional time-domain approaches, the analyzed results sometimes differ from the actual fluid transients. This discrepancy has been attributed to the fact that the conventional time-domain methods ignore frequency-dependent factors prevailing in actual systems such as friction, wave speed and dynamic characteristics of pipeline elements [3, 4]. The MOC, which uses the finite difference method for pipelines with these frequency-dependent factors, employs an iterative method to resolve these difficulties with a very small time step, resulting in a very time-consuming process.

Generally an unsteady flow consists of the steady harmonics related to the dynamic characteristics of a pipeline. For this reason, the frequency-domain approach is more practical and efficient in investigations of the individual contributions of pipeline elements. It focuses directly on the dynamic behavior of pipeline flow under oscillatory conditions [5-7].

The impulse response function (IRF) effectively describes the reaction of a pipeline when water hammer occurs [3, 4]. The IRF takes the form of the inverse Fourier transform (IFT) of the frequency response function (FRF) to obtain the system response. Unfortunately, with the IRF, the individual dynamic characteristics of pipeline elements, which include those of the inserted vibration element, cannot easily be identified, owing to the simple representation of the FRF.

In order to compensate for this disadvantage of the IRF approach, we expand the system FRF into partial fraction terms with an individual pole and its amplification constant. By this approach, the pole variation due to a frequency-dependent element in the pipeline can easily be observed. Additionally, the sum of the IFT results of partially fractioned terms delivers the final time-domain solution of a pipeline's unsteady flow. In the present study, we simulate the proposed approach using a simple pipeline incorporating an inserted vibration element.

† This paper was recommended for publication in revised form by Associate Editor Yeon June Kang
* Corresponding author. Tel.: +82 42 865 5372, Fax: +82 42 865 7804
E-mail address: ljs@kepri.re.kr

Moreover, we employ a graphical solution to express the physical behavior of the pressure wave in the simple pipeline, thereby validating our method.

## 2. Water hammer analysis in pipeline

### 2.1 Problem definitions

Fig. 1 shows the considered simple pipeline system, in which the fluid flow from a reservoir is suddenly blocked by a control valve. We could have installed in the pipeline a vibration element with mechanical impedance to mitigate the pressure fluctuation. In fact, we introduce a mathematical model of the vibration element as a piston-type or bladder-type accumulator. However, since this paper is dedicated to a mathematical approach to effective analysis of unsteady-flow pipelines, and since, therefore, the vibration element is just a simulation example for the proposed methodology, we do not devote much attention to the vibration element itself.

In the mathematical modeling, the coordinate $x$ runs from the reservoir through a pipeline of cross-sectional area $S$. We regard the control valve at $x = l$ as an unsteady flow source. It supplies virtually no velocity fluctuation to the pipeline under the system pressure $\boldsymbol{P}$ until the time reaches 0, after which it gradually increases the velocity fluctuation until $t = t_c$:

$$u_l(t) = \begin{cases} 0 & \text{when } t < 0, \\ \boldsymbol{U}(t/t_c) & \text{when } 0 < t < t_c, \\ \boldsymbol{U} & \text{when } t_c < t. \end{cases} \tag{1}$$

Generally, in fluid mechanics the pressure and the flow velocity are independent variables, whereas in linear acoustics they are dependent. The plus sign of the velocity fluctuation in Eq. (1) corrects for the discrepancy between the two physical fields.

The mechanical vibration element inserted into the pipeline has spring constant $K$, mass $M$, and cross-sectional area $S_M$. Hereafter, we use the subscript $M$ to represent the physical quantity of the vibration element.

The junction where the pipeline encounters the reservoir actually includes an acoustic impedance varying with frequency [8]. But we ignore this, because the area ratio of the pipeline to the reservoir is negligibly small, resulting in a force-free boundary condition at that point.

### 2.2 Governing equations

The continuity and momentum equations for the one-dimensional compressible fluid in the pipeline are [1, 2]

$$\frac{\partial p_x}{\partial t} + \rho c^2 \frac{\partial u_x}{\partial x} + \left[ u_x \frac{\partial p_x}{\partial x} \right] = 0 , \tag{2}$$

$$\frac{\partial u_x}{\partial t} + \frac{1}{\rho}\frac{\partial p_x}{\partial x} + \left[ u_x \frac{\partial u_x}{\partial x} + f \frac{u_x |u_x|}{2d} \right] = 0 . \tag{3}$$

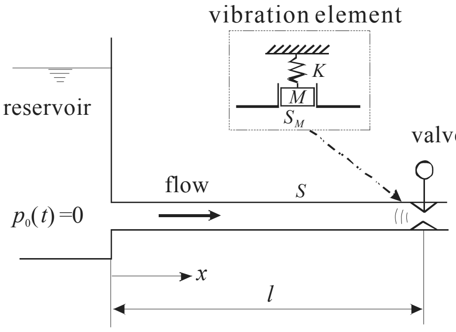


Fig. 1. Simple pipeline considered.

Here, $f$ and $d$ are the Darcy-Weisbach friction factor and the pipe diameter, respectively. For simplicity, we use $p_x$ and $u_x$ instead of $p_x(t)$ and $u_x(t)$.

For most engineering applications where $u_x / c << 1$, the convective terms $u_x \partial p_x / \partial x$ and $u_x \partial u_x / \partial x$ are very small compared with the other terms, and therefore are ignored. We also ignore the effect of the friction term $f u_x | u_x | / 2d$, in that the first oscillating peak is more dominant than the others where water hammer exists. Imposing these assumptions that ignore the convective terms braced by [ ] in Eqs. (1) and (2) yields the one-dimensional wave equation [9]

$$\frac{\partial^2 p_x(t)}{\partial t^2} = \frac{1}{c^2}\frac{\partial^2 p_x(t)}{\partial x^2} . \tag{4}$$

The Fourier transform of the pressure wave $p_x(t)$ yields the simple harmonic component as

$$P_x(\omega) = \int_{-\infty}^{\infty} p_x(t) e^{i\omega t} dt . \tag{5}$$

Table 1 shows the several Fourier transform results pertinent to the present study and noted, accordingly, throughout this paper.

Knowing all of the harmonic components, one can obtain the complete field by taking the IFT as

$$p_x(t) = \frac{1}{2\pi}\int_{-\infty}^{\infty} P_x(\omega) e^{-i\omega t} d\omega . \tag{6}$$

Incorporating Eq. (6) into (4) bears the well-known Helmholtz equation for a one-dimensional field:

$$\left[ \partial^2 / \partial x^2 + k^2 \right] P_x(\omega) = 0 . \tag{7}$$

In addition, substituting Eq. (6) for (2) and (3) produces the acoustic pressure and velocity relationships for a single frequency:

$$dU_x(\omega)/dx = (i\omega / \rho c^2) P_x(\omega) , \tag{8}$$

$$dP_x(\omega)/dx = i\omega\rho U_x(\omega) . \tag{9}$$

Table 1. Fourier transform pairs.

| Function | Fourier Transform |
|---|---|
| $f(t)$ | $F(\omega)=\int_{-\infty}^{\infty} f(t)e^{i\omega t}dt$ |
| $-\int_0^t\int_0^t f(t)dtdt$ | $F(\omega)/\omega^2$ |
| $f(t-a)$ | $e^{ia\omega}F(\omega)$ |
| $u(t)$ (unit-step function) | $-i/\omega$ |
| $\cos(at)u(t)$ | $\frac{-i\omega}{\omega^2-a^2}$ |
| $\frac{\cos(at)-1}{a^2}u(t)$ | $\frac{1}{\omega^2}\frac{-i\omega}{\omega^2-a^2}$ |
| $u_l(t)$ | $U_l(\omega)=\frac{\boldsymbol{U}}{t_c}\frac{1}{\omega^2}(e^{i\omega t_c-1})$ |

The 2nd-order differential equation in Eq. (7) yields the general solution [10]

$$P_x(\omega)=Ae^{ikx}+Be^{-ikx}, \tag{10}$$

and $\rho cU_x(\omega)$ can be obtained by Eqs. (8) and (9):

$$\rho cU_x(\omega)=Ae^{ikx}-Be^{-ikx}. \tag{11}$$

Considering the time harmonic to be $e^{i\omega t}$, $A$ and $B$ are the coefficients for left-going and right-going pressure waves, respectively. In the special case in which there are no reflections from the boundaries, Eqs. (10) and (11) deliver the relationship of the acoustic pressure and velocity at section $x$ as

$$p_x=\rho cu_x \text{ for propagating wave.} \tag{12}$$

### 2.3 Graphical solution for simple pipeline

If a pipeline end located at $x=0$ has a rigid boundary condition where $U_x(\omega)=0$, one can find that $A=B$ from Eq. (11). This means that the rigid boundary makes in-phase reflections for pressure waves and out-of-phase reflections for velocity waves. By contrast, the force-free boundary condition makes out-of-phase reflections for pressure waves and in-phase reflections for velocity waves. We should keep in mind that these physical laws for the simple boundaries explained at $x=0$ are applicable regardless of the location of the boundaries.

Given a pipeline with simple boundaries such as force-free or rigid boundaries, summation of the reflections from the boundaries provides a mathematically simple water hammer solution. This solution can be useful in effectively delivering physical meanings and in verifying computational results for more complex pipeline systems.

We assume that the pipeline shown in Fig. 1 has a force-free boundary at $x=0$ and a rigid boundary at $x=l$.

The first pressure wave abbreviated as ①, which is generated from the flow source and is described mathematically in Eqs. (1) and (12), travels under system pressure $\boldsymbol{P}$ to the left and arrives at $x$ when $t=(l-x)/c$, as shown in Fig. 2(a). The reflected wave abbreviated as ②, generated from the force-free boundary at $x=0$, runs out-of-phase with ① and arrives at $x$ when $t=(l+x)/c$. The third wave from the rigid boundary at $x=l$, expressed as ③, is added at $x$ when $t=[2l+(l-x)]/c$, and is in-phase with ②. In this mechanism, the boundaries send pressure waves periodically into the pipeline, the infinite sum of which, at $x$, yields the real pressure wave shown in Fig. 2(b). Examining the shape of this pressure wave, we can see that the pattern appears periodically.

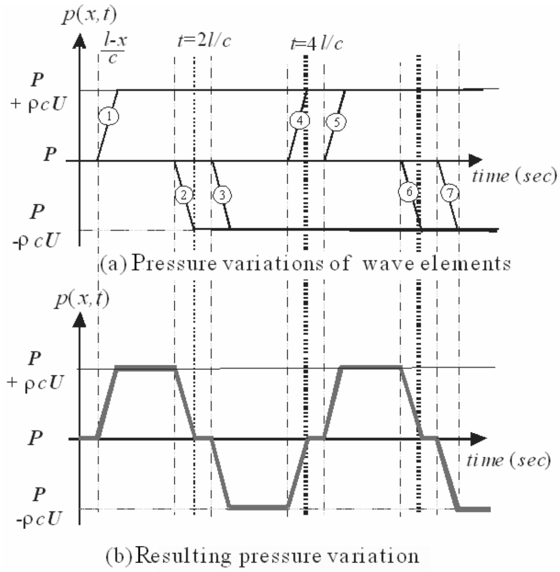


Fig. 2. Pressure wave variation at $x$ varying with time.

Generally, a pressure rise caused by water hammer is closely related to the valve-closing time $t_c$ and the round-trip-time of the wave-front in the pipeline $t_r=2l/c$. Fig. 3 plots pressure fluctuations at the flow source point for varying $t_c$. We can see that when $t_c<t_r$, the pressure waves always have a peak level of $\rho c\boldsymbol{U}$. In the opposite case, in which $t_c\geq t_r$, the waves always hold peak levels below $\rho c\boldsymbol{U}$. A longer duration of the valve-closing time can mitigate the water-hammer effect in the pipeline, as Fig. 3 shows.

### 2.4 Mathematical solution by proposed method without vibration element

First, we investigate pressure wave propagation for the simple case in which the pipeline end is under the force-free condition introduced in the graphical solution. Imposing the boundary conditions in Eqs. (10) and (11), we can derive the transfer function between the flow source and the section $x$ as

$$\frac{P_x}{U_l}=i\rho c\frac{\sin kx}{\cos kl}=i\rho c\frac{\sin \omega\frac{x}{c}x}{\cos\omega\frac{l}{c}}. \tag{13}$$

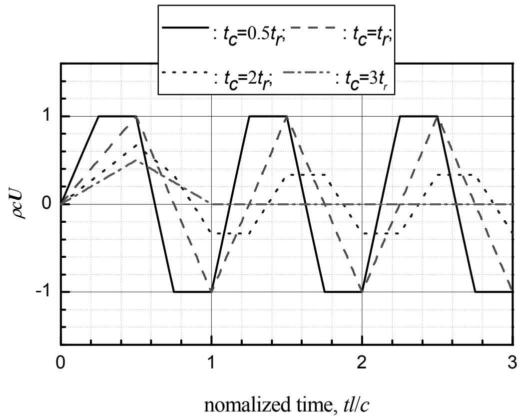


Fig. 3. Pressure fluctuations at $x = l$ varying with valve-closing time.

Inserting the Fourier transform of $U_l$ in Table 1 and rewriting the result yields

$$P_x = \rho c U \frac{1}{t_c}(e^{i\omega t_c} - 1)F_x \,, \tag{14}$$

where the function $F_x$ appears for mathematical convenience as

$$F_x = \frac{l^2}{c^2}\frac{i\sin kx}{(kl)^2\cos kl} = \frac{i\sin\omega\frac{x}{c}}{\omega^2\cos\omega\frac{l}{c}} \,. \tag{15}$$

The direct IFT of Eq. (14) agrees well with the graphical result presented in the previous section.

This mathematical process is straightforward and produces better results than input labor. However, since it does not consider the system characteristics, many physical instructions that can be useful for pipeline design might be ignored during in the computational process. In this context, this paper I ntroduces partial fraction expansion of the transfer function as an intermediate process preliminary to derivation of the final time-domain solution. The partial fraction expansion that is widely found in system analysis within the mechanical and electrical control fields utilizes the system poles that represent resonances.

We can easily determine that the $n$-th pole of Eq. (15) is $\omega_n = \pm 0.5\pi(2n-1)c/l$ . Decomposing $F_x$ into its poles yields

$$F_x = 2\frac{l}{c}\sum_{n=1}^{\infty} A_n \frac{-i\omega}{\omega^2(\omega^2 - \omega_n^2)} \,, \tag{16}$$

where the amplification factor of the n-th pole is given as

$$A_n = (-1)^{n-1}\frac{\sin(\omega_n \frac{x}{c})}{\omega_n^2} \,. \tag{17}$$

Taking the IFT of $F_x$, provided in Table 1, yields its time-domain expression

$$f_x(t) = 2\frac{l}{c}\sum_{n=1}^{\infty}[A_n \sin(\omega_n t) - 1] \,. \tag{18}$$

Then, we can finally derive the time-domain solution of $p_x(t)$ with Eq. (18) and the time delay Fourier transform of $e^{i\omega t_c}$ in Eq. (14) as

$$\frac{p_x(t)}{\rho c \boldsymbol{U}} = \frac{2l}{c t_c}\begin{cases} \sum_{n=1}^{\infty}[A_n \sin(\omega_n t) - 1] & 0 < t < t_c, \\ \sum_{n=1}^{\infty}\begin{Bmatrix} A_n \cos[\omega_n (t - t_c)] \\ -\cos(\omega_n t) \end{Bmatrix} & t > t_c. \end{cases} \tag{19}$$

The partial fraction expansion of the transfer function perhaps looks more complicated than the direct one. However, it provides the useful physical information that the time-domain response in a pipeline under water hammer is comprised of infinite acoustic modes multiplied by their amplification factors.

### *2.5 Mathematical solution by proposed method for pipe with simple vibration element*

Based on the heretofore-derived results, we can extend the application of the proposed approach to a pipeline including a vibration element. A simple vibration element inserted into a pipeline section changes the dynamic characteristics of the simple pipeline: poles, mode shapes and amplification factors. Accordingly, we investigated the effect of inserting a vibration element by examining changes in the dynamic characteristics.

For a simple description, it is convenient to introduce a specific acoustic impedance for a single frequency as

$$z = \frac{P_x}{\rho c U_x} \,. \tag{20}$$

With this notation, we obtain the specific acoustic impedance for the vibration element as

$$z_M = i\frac{K - M\omega^2}{\rho c \omega S_M} = i\frac{M}{\rho l S_M}\frac{(\omega_M l/c)^2 - (kl)^2}{kl} \,, \tag{21}$$

where the natural frequency of the vibration element can be written as $\omega_M = \sqrt{K/M}$ .

Since most devices for mitigation of flow fluctuation are located near the control valve, we ignore the clearance between the flow source and the vibration element. With this assumption and Eq. (13), superposing the solutions of the flow source and the vibration element yields the fluid pressure at section $x$

$$P_x = i\rho c \frac{\sin kx}{\cos kl}(U_l + \tilde{S}U_M) \,, \tag{22}$$

where $U_M$ is the particle velocity of the vibration element and $\tilde{S}$ designates the sectional area ratio of the vibration element to the pipeline as $\tilde{S} = S_M / S$ .

By imposing the continuity condition of fluid pressure and Eq. (21), we can obtain the fluid pressure at section $x$ for a single frequency in the form of Eq. (14), only changing $F_x$ as

$$F_x = \frac{l^2}{c^2} \frac{i z_M \sin kx}{(kl)^2 [z_M \cos kl + i\tilde{S} \sin kl]} . \quad (23)$$

The poles occur when the denominator in Eq. (23) vanishes, resulting in

$$\tan kl = \frac{\tilde{M}}{\tilde{S}} \frac{(kl)^2 - (\omega_M l / c)^2}{kl} , \quad (24)$$

$$\tilde{M} = M / (\rho S_M l) , \quad (25)$$

where $\tilde{M}$ is the ratio of $M$ to the effective pipeline inertia.

Since there is no explicit solution to this transcendental equation, the graphical representation in Fig. 4 will aid understanding of the pole change as effected by the vibration element. The intersections of the left-side and right-side functions in Eq. (24) hold the poles of the pipeline. From Eq. (24) and the graphical representations, we can easily determine that when the area ratio approaches 0 or the spring constant of the vibration element is so large that it can be assumed to be rigid, the vibration element cannot change the dynamic characteristics of the simple pipeline. However, in the case that $0 < \omega_M l / c < \pi$ and an appropriate constant $\tilde{M}$ is applied to the pipeline, the first resonance disappears owing to the presence of the vibration element, as shown in Fig. 4.

Differentiating the denominator of Eq. (23) with respect to $kl$ and substituting $kl$ for the $n$-th pole $(kl)_n$ yields the residue

$$A_n = \frac{\frac{l^2}{c^2} \sin[(kl)\frac{x}{l}]}{(kl)^2 \sin kl} \frac{\tilde{M}^2 D^2}{\tilde{M}^2 D^2 + \tilde{M}\tilde{S}E - \tilde{S}^2 \tilde{M}^2} , \quad (26)$$

where

$$D = \left(\frac{\omega_M l}{c}\right)^2 - (kl)^2 , \ E = \left(\frac{\omega_M l}{c}\right)^2 + (kl)^2 . \quad (27)$$

Finally, the pressure wave $p_x(t)$ can be derived by substituting the changed poles and their amplification factors into Eq. (19). When $\tilde{M}$ goes to infinity or $\tilde{S}$ to zero, we find that the solid line in Fig. 5 represents a result without a vibration element and is identical to the graphical solution depicted in Fig. 3.

Fig. 5 shows that an appropriate design of the vibration element reduces the water-hammer pressure in the pipeline where the vibration element has the same values used in Fig. 4.

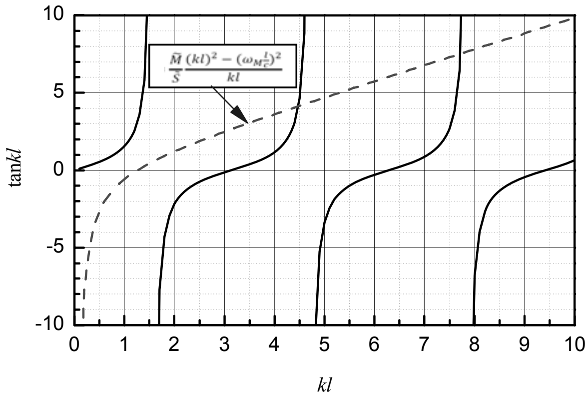


Fig. 4. Graphical solution of Eq. (24) when $\tilde{M} = \tilde{S} = 0.1$ and $\omega_M l / c = 0.8$ .

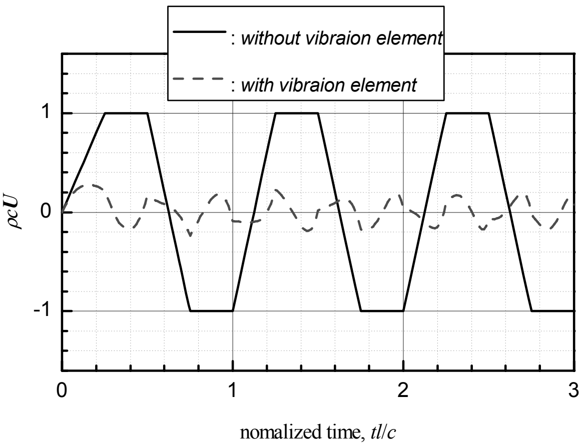


Fig. 5. Comparison of results of pressure waves with and without vibration element in pipe.

## 3. Conclusions

For effective analysis of water hammer occurring in a pipeline, we have proposed partial fraction expansion of the transfer function as an intermediate process preliminary to the final time-domain solution. With this approach, in contrast to the conventional time-domain methods, we could employ a vibration element to simply analyze changes of the dynamic characteristics of pipeline flow. Moreover, our simulated results yielded much physical information applicable to the design of innovative pipeline elements.

One of the insights gained is that locating the resonance of the vibration element between the first and second resonances of the pipeline can reduce the abrupt rise of pressure incident on the occurrence of water hammer. It is expected that our method of partial fraction expansion will prove useful to researchers analyzing unsteady flow in pipelines.

## Nomenclature

$\rho$ : Fluid density

$\omega$ : Angular frequency

$c$ : Wave speed in fluid
$k$ : Wave-number in fluid
$u(t)$ : Unit-step function
$u_x(t)$, $U_x$ : Particle velocity at time $t$ and at $x$
$U_x(\omega)$, $U_x$ : Single frequency component of $u_x(t)$
$\boldsymbol{U}$ : Operating velocity in pipeline
$p_x(t)$, $p_x$ : Pressure wave at time $t$ and at $x$
$P_x(\omega)$, $P_x$ : Single frequency component of $p_x(t)$
$\boldsymbol{P}$ : Operating pressure in pipeline
$t$ : Time variable
$t_c$ : Valve closing time
$t_r$ : Reciprocal of pipeline natural frequency
$z$ : Specific acoustic impedance

## References

[1] V. L. Streeter and E. B. Wylie, *Hydraulic transients*, McGraw-Hill, New York, USA (1967).
[2] E. B. Wylie and V. L. Streeter, *Fluid transient in systems, Prentice Hall Inc.*, Englewood Cliffs, N. J. (1993).
[3] L. Suo and E. B. Wylie, Impulse response method for frequency-dependent pipeline transients, *Journal of Fluids Engineering*, 111 (4) (1989) 478-483.
[4] S. H. Kim, Design of surge tank for water supply systems using the impulse response method with the GA algorithm, *Journal of Mechanical Science and Technology*, 24 (2) (2010) 629-638.
[5] B. Brunone and M. Ferrante, Detecting leaks in pressurized pipes by means of transient, *J. Hydraul. Res.* 39 (5) (2001) 539-547.
[6] W. Mpesha M. H. Chaudhry, and Gassman S, Leak detection in pipes by frequency response method using a step excitation, *J. Hydraul. Res.* 40 (1) (2002) 55-62.
[7] M. Ferrante and B. Brunone, Pipe system diagnosis and leak detection by unsteady-state tests–1: harmonic analysis, *Adv. Water Resour.* 26 (2002) 95-105.
[8] P. M. Morese and K. U. Ingard, *Theoretical Acoustics* (Chap. 7), McGraw-Hill, New York, USA (1968).
[9] L. E. Kinsler et al., *Fundamentals of Acoustics* (Chap. 5), John Wiley & Sons, New York, USA (1982).
[10] M. L. Munsal, *Acoustics of Ducts and Mufflers* (Chap. 1), John Wiley & Sons, New York, USA (1987).

**Jun-Shin Lee** received his Ph. D. degree from the Mechanical Engineering Department of KAIST in 1995. He is currently a principal researcher in the Green-Growth Laboratory of the Research Institute in the Korea Electric Power Corporation, Daejeon, Korea. His research interests are the vibration control of pipelines built in nuclear power plants and development of predictive monitoring algorithms for wind turbines.

**Bong-Ki Kim** received his Ph. D. degree in 1997 from the Department of Mechanical Engineering of KAIST. He was a research engineer in the NVH department at the Samsung Motors Technology Center from 1997 to 1998. From 1999 to 2000, he worked at Arvin-Meritor Exhaust in the USA as a research engineer. Since 2000, he has been working with the acoustics research group of KIMM. His research interests include sound field visualization and noise/vibration control.

**Wook-Ryun Lee** received his Master's degree in Mechanical Engineering from Chungnam National University in 2004. He is currently a senior researcher in the Power Generation Laboratory of the Research Institute of the Korea Electric Power Corporation, Daejeon, Korea. His research interests are control of noise and vibration generated from power plants, and electrical energy storage using superconducting flywheels.

**Ki-Yong Oh** received his Master's degree in Mechanical Engineering Department from KAIST in 2006. He is currently a researcher in the Green-Growth Laboratory of the Research Institute of the Korea Electric Power Corporation, Daejeon, Korea. His research interests include active control of vibration and wind turbine design.